# xuv-laser spectroscopy of HD at 92-98 nm

P. C. Hinnen,[1,2] S. E. Werners,[1] S. Stolte,[2] W. Hogervorst,[1] and W. Ubachs[1]

[1]*Department of Physics and Astronomy, Laser Centre Vrije Universiteit, De Boelelaan 1081, 1081 HV Amsterdam, Netherlands*

[2]*Department of Chemistry, Laser Centre Vrije Universiteit, De Boelelaan 1083, 1081 HV Amsterdam, Netherlands*

Sub-Doppler excitation spectra of HD have been recorded in the range 92-98 nm with the use of a narrow-band and tunable extreme ultraviolet laser in combination with a molecular beam. Frequencies of 147 transitions to the $B\ ^1\Sigma_u^+$, $C\ ^1\Pi_u$, and $EF\ ^1\Sigma_g^+$ states have been calibrated with an average absolute accuracy of 0.035 cm$^{-1}$. The data have been analyzed in the framework of a semiempirical deperturbation model involving mutual couplings between nearby lying levels of the $B\ ^1\Sigma_u^+$ and $C\ ^1\Pi_u$ states. Also, symmetry-breaking effects, i.e., interactions with $EF\ ^1\Sigma_g^+$ gerade states, were inferred from the data.

PACS number(s): 33.20.Ni, 42.65.Ky, 07.60.Rd

## I. INTRODUCTION

The spectroscopy of molecular hydrogen and its isotopes has, throughout the years, attracted much interest for the obvious reason that hydrogen is the simplest neutral molecule. *Ab initio* calculation of the equilibrium bond length, dissociation, and ionization energies, as well as level energies, can be performed with high precision [1-4]. A challenging obstacle in these calculations is that effects beyond the Born-Oppenheimer approximation are more important for hydrogen than for any other molecule, due to the small mass of the nuclei. Nonadiabatic effects were found to cause shifts in the rovibrational energies of $B\ ^1\Sigma_u^+$ and $C\ ^1\Pi_u$ states of $H_2$ of over 10 cm$^{-1}$ [5-7].

A study of the HD spectrum does not only yield information on reduced mass effects, as commonly studied via isotopic substitution in molecular spectroscopy. Within the framework of the Born-Oppenheimer approximation HD is treated as a homonuclear molecule obeying $g,u$ symmetry rules, but in a more rigorous treatment the $g,u$ symmetry breaks down, giving rise to phenomena not observed in $H_2$ or $D_2$. In contrast to $H_2$ and $D_2$, the HD molecule has an infrared dipole spectrum [8], surpasses the ortho-para symmetry rules, and the dissociation limit splits into two components corresponding to H*+D and H+D* channels [9]. Of relevance for the present work is that in HD, apart from the $B\ ^1\Sigma_u^+$ and $C\ ^1\Pi_u$ states, also the $EF\ ^1\Sigma_g^+$ state can be excited in a one-photon transition. This $EF\ ^1\Sigma_g^+$ state is coupled to the $B\ ^1\Sigma_u^+$ and $C\ ^1\Pi_u$ states, giving rise to additional perturbations. This is not the case for the homonuclear hydrogen isotopomers.

The electronic absorption spectrum of hydrogen starts near 100 nm and extends to shorter wavelengths. The spectroscopic data obtained in large classical spectrographs have long stood as the most accurate, because narrow-band and tunable laser sources were not available in this wavelength range. For the spectroscopy of the electronically excited states of HD the report on the vacuum ultraviolet absorption and emission spectrum by Dabrowski and Herzberg [10] is the most extensive and detailed. Only in recent years have lasers and laser techniques become sufficiently sophisticated to improve upon the accuracy of classical spectrometers,

even for the highly excited states. Transition frequencies of selected levels in the $EF\ ^1\Sigma_g^+$ state of HD were determined by Doppler-free two-photon absorption using an uv laser [11]. This work was further extended to yield an accurate ionization potential of HD [12]. In another experiment a narrow-band xuv-laser source was used to determine the dissociation limits in HD [13]. In the present work on the excitation spectroscopy of HD in the range 92-98 nm a similar coherent xuv source is employed. Transition frequencies of rotational lines in the $B\ ^1\Sigma_u^+ - X\ ^1\Sigma_g^+ (v',0)$ bands for $v' = 12-14$ and 16-19; the $C\ ^1\Pi_u - X\ ^1\Sigma_g^+ (v',0)$ bands for $v' = 2$, 4, and 5; and the $EF\ ^1\Sigma_g^+ - X\ ^1\Sigma_g^+ (v',0)$ bands for $v' = 5-8$ and 10-14 were calibrated with a mean accuracy of 0.035 cm$^{-1}$. Although the wavelength coverage is not as broad as in the work of Dabrowski and Herzberg [10], the present accuracy is a factor of 5 higher. The data were analyzed in a semiempirical deperturbation model in which mutual couplings between the $B\ ^1\Sigma_u^+$, $C\ ^1\Pi_u$, and $EF\ ^1\Sigma_g$
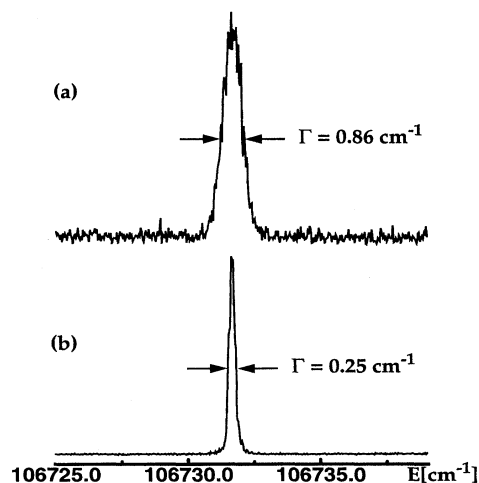


FIG. 1. $C(4\text{-}0)\ R(0)$ transition of HD, measured (a) in background gas and (b) in the molecular-beam expansion. The width in the upper spectrum is the convolution of Doppler width and the bandwidth of the xuv source, while in the lower spectrum the xuv source bandwidth determines the observed width.
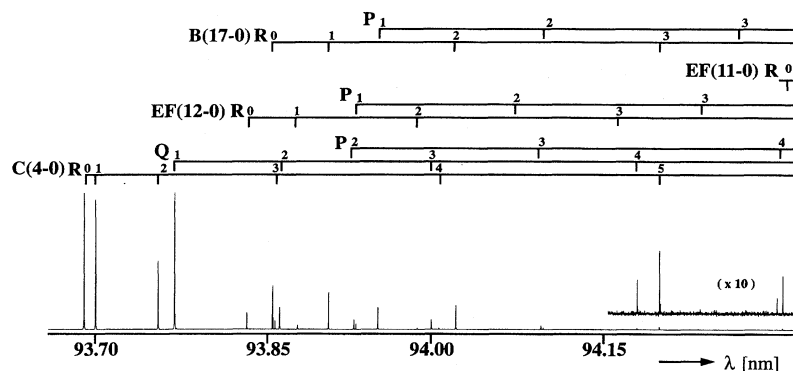
FIG. 2. Overview spectrum of HD in the wavelength range 93.7–94.3 nm. Note the differences in intensity of $R(0)$ lines in the $EF$-$X$ (12,0) and (11,0) bands. As the bandhead of the former band is very close to the $B$-$X$(17,0) band, the lower $J$ states are severely mixed, giving rise to intensity-borrowing effects resulting in a relatively strong $EF$-$X$(12,0) band.

excited states are taken into account.

## II. EXPERIMENT

The setup of the xuv-laser source was described before in some detail [14] and its specific application to high-resolution spectroscopy on $H_2$ was documented as well [15]. In short, narrow-band radiation in the xuv range 92–98 nm was produced via third-harmonic generation of a frequency-doubled pulsed dye laser in a pulsed jet of xenon gas. The xuv radiation is forwardly directed in a confined beam, spa-

tially and temporally overlapping the incident intense uv beam at three times its wavelength. The HD molecules are excited by the xuv in a crossed molecular-beam–laser-beam geometry. Resonances of HD are measured via 1 xuv +1 uv ionization with the detection of $HD^+$ ions after a time-of-flight mass selecting zone. As the bandwidth of the xuv source is about 0.22–0.25 cm$^{-1}$, sub-Doppler measurements are feasible in this setup. In Fig. 1 a comparison of a sub-Doppler spectrum, recorded from the molecular beam, and a Doppler broadened spectrum, recorded in low-density background gas, is shown. As the residual Doppler broadening in the beam setup, due to the divergences of the molecu-lar and the xuv beam, is below 0.02 cm$^{-1}$, the linewidth in the first case is fully determined by the bandwidth of the light source. In the latter case the observed linewidth of 0.86 cm$^{-1}$ is a convolution of the Doppler width (0.71 cm$^{-1}$ at room temperature for HD near 100 nm) and the bandwidth of the source.

Precise calibration of the absolute transition frequencies was performed against the $I_2$ absorption standard [16]. Exci-
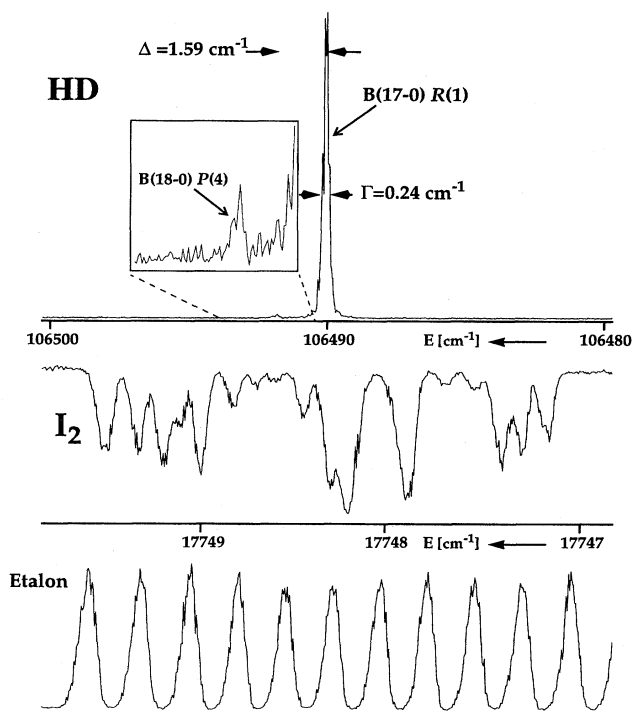


FIG. 3. Upper spectrum: high-resolution recording of a previously unresolved blending of two spectral components in HD at $\sim 106\,490$ cm$^{-1}$. A weak feature, assigned as the $P(4)$ line of the $B$-$X$ (18,0) band, is now well separated from a strong feature assigned as the $R(1)$ line of the $B$-$X$(17,0) band. Also shown are the $I_2$ absorption spectrum (middle trace) and étalon fringes (lower trace), recorded at the fundamental frequency, used for calibration purposes. All data points were averaged over four laser shots.
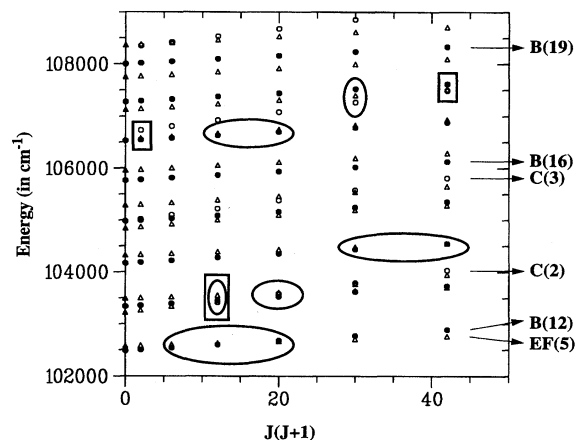


FIG. 4. Energy-level diagram of HD in the relevant energy range of the present experiment. Rotational quantum states in $B\ ^1\Sigma_u^+$ are indicated by ●, states of $C\ ^1\Pi$ by ○, and states of $EF\ ^1\Sigma_g^+$ by △. Local perturbations, which were analyzed in this work, are indicated by square or elliptical shapes. The squares refer to heterogeneous interactions between $B$ and $C$ levels. The elliptical features involve couplings with $EF$ levels; horizontal ellipses represent homogeneous couplings to $B$ levels and vertical ellipses represent heterogeneous couplings to $C$ levels.

TABLE I. Observed transition frequencies of the $B\ ^1\Sigma_u^+ - X\ ^1\Sigma_g^+$ ($v'$,0) Lyman bands of HD. The value in parentheses represents the uncertainty in the last digit. For the (13,0) band no successful deperturbation analysis could be performed. $\Delta_{OC}$ refers to the difference between present observations and the levels calculated from the deperturbation analysis. $\Delta_{OD}$ lists the differences between the observed frequencies and those of Ref. [10]. All values are given in cm$^{-1}$.

| $J$ | $R(J)$ | $\Delta_{OC}$ | $\Delta_{OD}$ | $P(J)$ | $\Delta_{OC}$ | $\Delta_{OD}$ |
|---|---|---|---|---|---|---|
| | | | (19-0) band | | | |
| 0 | 108 017.23(3) | $-0.00$ | $+0.58$ | | | |
| 1 | 107 959.36(3) | $-0.01$ | $-0.51$ | 107 912.37(3) | $+0.03$ | $+0.56$ |
| 2 | 107 828.53(4) | $+0.01$ | $+0.48$ | 107 750.19(3) | $-0.00$ | $+0.50$ |
| 3 | 107 625.85(4) | $+0.03$ | $+0.45$ | 107 516.20(3) | $-0.09$ | $+0.40$ |
| 4 | 107 353.03(4) | $-0.01$ | $+0.51$ | 107 212.37(5) | $-0.05$ | $+0.37$ |
| | | | (18-0) band | | | |
| 0 | 107 293.01(3) | $+0.00$ | $+0.20$ | | | |
| 1 | 107 236.56(3) | $-0.01$ | $+0.22$ | 107 187.38(3) | $+0.00$ | $+0.22$ |
| 2 | 107 107.91(5) | $+0.04$ | $+0.25$ | 107 025.94(3) | $-0.01$ | $+0.17$ |
| 3 | 106 908.14(3) | $+0.00$ | $+0.29$ | 106 793.50(3) | $-0.00$ | $+0.28$ |
| 4 | 106 641.2(1) [a] | | | 106 491.70(6) | $-0.09$ | $+0.8$ [b] |
| 5 | 106 306.00(5) | $+0.01$ | $+0.66$ | | | |
| | | | (17-0) band | | | |
| 0 | 106 546.15(4) | $+0.05$ | $+0.47$ | | | |
| 1 | 106 490.11(3) | $+0.01$ | $-0.83$ | 106 440.31(4) | $-0.02$ | $+0.15$ |
| 2 | 106 362.19(3) | $+0.00$ | $-0.79$ | 106 279.04(3) | $-0.01$ | $+0.50$ |
| 3 | 106 162.3(1) [c] | $+0.1$ | $-0.8$ | 106 047.05(5) | $+0.01$ | d |
| 4 | | | | 105 746.09(3) | $-0.01$ | $+0.34$ |
| | | | (16-0) band | | | |
| 0 | 105 781.73(3) | $+0.01$ | $+0.19$ | | | |
| 1 | 105 727.12(3) | $-0.01$ | $-0.77$ | 105 675.13(3) | $-0.02$ | $-0.18$ |
| 2 | 105 601.12(4) | $+0.01$ | $+0.59$ | 105 514.67(3) | $+0.00$ | $-0.03$ |
| 3 | 105 404.66(4) | $+0.00$ | $-0.14$ | 105 284.06(3) | $-0.00$ | $-0.20$ |
| | | | (14-0) band | | | |
| 0 | 104 186.29(3) | $+0.02$ | $-0.19$ | | | |
| 1 | 104 133.61(3) | $-0.03$ | $-0.04$ | 104 078.74(3) | $+0.01$ | $-0.03$ |
| 2 | 104 010.55(3) | $+0.04$ | $-0.17$ | 103 919.20(3) | $-0.02$ | $-0.41$ |
| 3 | 103 817.96(5) | $+0.07$ | $-0.13$ | 103 690.57(3) | $-0.00$ | $-0.26$ |
| 4 | 103 557.04(3) | $+0.01$ | $-0.24$ | 103 394.43(3) | $+0.00$ | $-0.10$ |
| 5 | e | | | 103 032.84(5) | $-0.05$ | $-0.71$ |
| 6 | 102 842.87(4) | $-0.00$ | f | 102 608.20(3) | $-0.02$ | $--0.08$ |
| | | | (13-0) band | | | |
| 0 | 103 356.44(3) | | $-0.26$ | | | |
| 1 | 103 305.97(3) | | $-0.29$ | 103 247.99(2) | | $-0.31$ |
| 2 | 103 191.65(3)[g] | | $+0.03$ | 103 089.31(3) | | $-0.55$ |
| 3 | 102 985.10(3) | | $-0.04$ | 102 862.79(3) | | $-0.35$ |
| 4 | 102 725.67(3) | | $-0.38$ | 102 575.47(3)[g] | | $-0.09$ |
| 5 | 102 409.31(3) | | $-0.10$ | 102 200.12(3) | | $+0.16$ |
| 6 | 102 022.76(4) | | $-0.06$ | | | |
| | | | (12-0) band | | | |
| 0 | 102 503.56(3) | $+0.01$ | $+0.66$ | | | |
| 1 | 102 453.07(3) | $-0.00$ | $-0.40$ | 102 394.87(3) | $-0.02$ | $-0.49$ |
| 2 | 102 332.86(3) | $+0.01$ | $-0.30$ | 102 236.52(3) | $+0.03$ | $-0.28$ |
| 3 | | | | 102 009.95(4) | $-0.06$ | $-0.20$ |

[a]Blended by $C(4-0)Q(1)$.
[b]Blended in Ref. [10].
[c]Blended by $C(4-0)R(5)$.
[d]Overlapped by strong emission lines in the source in Ref. [10].
[e]Lines observed at 103 221.6(9), 103 229.3(5), and 103 235.71(3) cm$^{-1}$, respectively, but none of these could be unambiguously assigned as $R(5)$.
[f]Not observed in Ref. [10].
[g]Ambiguous assignment of the $P(4)$-$R(2)$ pair; might be assigned as belonging to the $EF$-$X(6,0)$ band.

TABLE II. Observed transition frequencies of the $C\ ^1\Pi_u - X\ ^1\Sigma_g^+$ $(v',0)$ Werner bands of HD. The value in parentheses represents the uncertainty in the last digit. $\Delta_{OC}$ refers to the difference between present observations and the frequencies calculated from the deperturbation analysis. For the (2,0) band no successful deperturbation analysis could be performed. $\Delta_{OD}$ lists the difference between the observed transition frequencies and those of Ref. [10]. All values are given in $cm^{-1}$.

| $J$ | $R(J)$ | $\Delta_{OC}$ | $\Delta_{OD}$ | $Q(J)$ | $\Delta_{OC}$ | $\Delta_{OD}$ | $P(J)$ | $\Delta_{OC}$ | $\Delta_{OD}$ |
|---|---|---|---|---|---|---|---|---|---|
| | | | | (5-0) band | | | | | |
| 4 | 107 961.87(4) | | +0.76 | 107 786.40(5) | | +0.57 | | | |
| 5 | | | | | | | 107 356.88(4) | | +0.16 |
| | | | | (4-0) band | | | | | |
| 0 | 106 731.58(3) | +0.00 | −0.01 | | | | | | |
| 1 | 106 719.92(3) | +0.02 | +0.08 | 106 641.20(3) [a] | +0.00 | +0.15 | | | |
| 2 | 106 657.21(3) | +0.01 | +0.03 | 106 538.98(3) | +0.00 | +0.10 | 106 464.51(3) | −0.01 | +0.36 |
| 3 | 106 543.58(3) | +0.01 | +0.15 | 106 386.56(3) | −0.02 | +0.04 | 106 276.83(3) | −0.00 | +0.08 |
| 4 | 106 379.18(4) | −0.01 | +0.26 | 106 185.15(5) | +0.05 | +0.46 | 106 041.10(3) | −0.02 | −0.32 |
| 5 | 106 163.42(4) [b] | +0.04 | +0.49 | 105 935.94(4) | −0.01 | +0.41 | 105 758.55(3) | −0.01 | +0.33 |
| | | | | (2-0) band | | | | | |
| 0 | 103 202.08(2) | | −0.05 | | | | | | |
| 1 | 103 196.82(4) | | −0.13 | 103 112.34(3) | +0.03 | −0.40 | | | |
| 2 | 103 140.28(3) | | −0.32 | 103 017.85(5) | −0.06 | −0.13 | 102 934.86(3) | | +0.18 |
| 3 | 103 056.64(5) | | −0.05 | 102 877.17(4) | −0.06 | −0.15 | 102 753.59(3) | | −0.39 |
| 4 | 102 909.45(3) | | −0.63 | 102 691.33(3) | +0.02 | −0.17 | 102 524.15(3) | | −0.07 |
| 5 | 102 719.78(3) | | −0.03 | 102 461.54(3) | +0.02 | −0.15 | 102 271.66(3) | | −0.05 |
| 6 | 102 486.29(3) | | −0.14 | 102 189.45(4) | −0.01 | +0.33 | 101 960.76(4) | | +0.36 |

[a]Blending $B(18\text{-}0)R(4)$.
[b]Blending $B(17\text{-}0)R(3)$.

tation spectra of HD in the xuv range and the absorption spectrum of $I_2$ in the visible were recorded simultaneously with the sixth harmonic and fundamental wavelength of the dye laser. Via computerized fitting with Gaussian line shapes, interpolation of the wavelength scale, and subsequent multiplication of the result by a factor 6, the transition frequencies of the HD lines were determined. Before the interpolation procedure the wavelength scale was linearized with the use of an étalon marker spectrum, also recorded in the visible. Finally, a correction for a misalignment of the crossed beams, resulting in a small Doppler shift (about 0.01 $cm^{-1}$), was made. The recalibration of the $I_2$ atlas [17] was accounted for. In the error budget the errors due to the inaccuracy of the iodine atlas (0.006 $cm^{-1}$ at the sixth harmonic), the uncertainty in the Doppler shift (0.005 $cm^{-1}$), the error from the interpolation procedure (average 0.01 $cm^{-1}$), and the error due to the noise on the lines (average 0.01 $cm^{-1}$) were included. After averaging the results of at least three recordings for each resonance a total error ranging from 0.02 to 0.08 $cm^{-1}$ with a mean of 0.035 $cm^{-1}$ is found. For more details on these procedures we refer to Ref. [15].

### III. RESULTS AND DISCUSSION

In Fig. 2 an overview excitation spectrum of HD in the wavelength range 93.7–94.3 nm is shown. The spectrum covers the bandhead region of the $C$-$X(4,0)$, $B$-$X(17,0)$, and $EF$-$X(12,0)$ bands. At the long-wavelength side, the $R(0)$ line of the $EF$-$X(11,0)$ band appears as well at a much lower intensity than the $R(0)$ line of the $EF$-$X(12,0)$ band. The

intensity in the $EF$-$X$ system is expected to be much weaker than in $B$-$X$ and $C$-$X$ systems as it is a forbidden transition in the Born-Oppenheimer approximation. The increased intensity of the EF-$X(12,0)$ band is an indication of a coupling between $B\ ^1\Sigma_u^+$ and $EF\ ^1\Sigma_g^+$ states, giving rise to an intensity borrowing effect. After taking overview spectra as presented in Fig. 2, an energy range of at least 20 $cm^{-1}$ around each resonance was recorded, allowing reliable linearization and calibration procedures using the etalon and $I_2$ absorption spectra.

In Fig. 3 simultaneous recordings of a HD excitation spectrum of the $B$-$X(17,0)$ $R(1)$ line with the $I_2$ and étalon calibrations are shown. In previous studies with Doppler limited resolution this HD resonance was suspected to consist of more unresolved lines. Due to the sub-Doppler resolution of the present experiment the weak $B$-$X(18,0)$ $P(4)$ line can be separated from the intense $B$-$X(17,0)$ $R(1)$ line. The results obtained for transition frequencies of calibrated rotational lines are given in Tables I–III for the $B$-$X$, $C$-$X$, and $EF$-$X$ systems, respectively.

The assignment of the HD resonances is complicated by the strong mutual perturbations between the excited states. Only the $(f)$ components of the $C\ ^1\Pi_u$ state follow an unperturbed rotational progression. An important handle in the assignment is the use of combination differences, i.e., the frequency difference between corresponding $R(J)$ and $P(J + 2)$ lines, that should match known $X\ ^1\Sigma_g^+$ ground-state energy differences. Line intensities cannot be reliably used because of the intensity borrowing phenomena near local

TABLE III. Observed transition frequencies of the $EF\,^1\Sigma_g^+ - X\,^1\Sigma_g^+$ $(v',0)$ bands of HD. The value in parentheses represents the uncertainty in the last digit. $\Delta_{OC}$ refers to the difference between present observations and the frequencies calculated from the deperturbation analysis. For the (11,0) and (10,0) bands not enough data were obtained to perform a rotational analysis. For the (7,0) and (6,0) bands attempts to perform a deperturbation analysis were unsuccessful. $\Delta_{OD}$ lists the difference between the observed transition frequencies and those of Ref. [10]. All values are given in cm$^{-1}$.

| $J$ | $R(J)$ | $\Delta_{OC}$ | $\Delta_{OD}$ | $P(J)$ | $\Delta_{OC}$ | $\Delta_{OD}$ |
|---|---|---|---|---|---|---|
| | | | (14-0) band | | | |
| 0 | 107 766.74(3) | | +0.71 | | | |
| 1 | 107 710.47(8) | | +0.43 | 107 661.13(5) | | −0.02 |
| | | | (13-0) band | | | |
| 0 | 107 143.07(4) | −0.02 | +0.42 | | | |
| 1 | 107 090.27(3) | −0.02 | +0.31 | 107 035.74(6) | −0.04 | +0.47 |
| 2 | 106 967.44(6) | −0.03 | +0.30 | 106 875.90(6) | −0.09 | +0.38 |
| | | | (12-0) band | | | |
| 0 | 106 571.32(5) | −0.05 | +0.28 | | | |
| 1 | 106 521.16(4) | +0.03 | +0.33 | 106 462.48(4) | −0.02 | −0.33 |
| 2 | 106 400.64(5) | −0.00 | +0.66 | 106 304.31(4) | −0.05 | +0.42 |
| | | | (11-0) band | | | |
| 0 | 105 979.44(4) | | a | | | |
| 1 | 105 921.32(3) | | +0.36 | | | |
| | | | (10-0) band | | | |
| 0 | 105 301.33(4) | | −0.20 | | | |
| 1 | 105 247.11(5) | | −0.55 | | | |
| | | | (8-0) band | | | |
| 0 | 104 340.14(3) | −0.02 | −0.22 | | | |
| 1 | 104 272.23(3) | +0.02 | +0.04 | | | |
| 2 | 104 125.66(3) | −0.03 | +2.33 | 104 073.10(3) | −0.00 | −0.11 |
| 3 | 103 901.11(3) | +0.01 | −0.65 | 103 829.15(4) | +0.00 | +0.25 |
| | | | (7-0) band | | | |
| 0 | 103 503.57(3) | | −0.04 | | | |
| 1 | 103 434.54(4) | | +0.33 | 103 404.6(1) [b] | | +0.13 |
| 2 | 103 292.70(3) | | +0.10 | c | | −0.11 |
| 3 | 103 026.13(3) | | −0.18 | 102 991.31(4) | | −0.09 |
| 4 | 102 736.44(4) | | −0.42 | 102 676.46(4) | | d |
| | | | (6-0) band | | | |
| 0 | 103 263.2(7) | | d | | | |
| 1 | 103 254.4(3) [b] | | | 103 120.3(3) [b] | | d |
| 2 | 103 189.08(3) [e] | | −0.38 | | | |
| 3 | | | | | | |
| 4 | 102 885.7(2) [b] | | d | 102 572.96(3) [e] | | 0.14 |
| | | | (5-0) band | | | |
| 0 | 102 586.21(3) | +0.03 | +0.12 | | | |
| 1 | 102 514.73(3) | −0.01 | −0.01 | 102 488.05(3) | −0.01 | +0.00 |
| 2 | 102 363.76(3) | +0.00 | +0.04 | 102 319.10(3) | −0.02 | +0.01 |
| 3 | 102 130.99(3) | +0.00 | +0.01 | 102 071.60(7) | −0.07 | +0.31 |

[a]Overlapped by strong emission lines in the source in Ref. [10].

[b]Very weak lines observed at low signal-to-noise ratio.

[c]Line observed at 103 235.71(2), but this frequency does not agree with combination difference $P(2)-R(0)=267.07(3)$ cm$^{-1}$.

[d]Not observed in Ref. [10].

[e]Ambiguous assignment of $P(4)-R(2)$ pair; might be assigned as belonging to the $B$-$X(13,0)$ band.

TABLE IV. Band origin $\nu_0^v$, rotational constants $B_v$, $D_v$, and deperturbation parameters in the $B\,^1\Sigma_u^+$ state of HD, as calculated from the analysis. The value in parentheses represents the uncertainty in the last digit. All values are in cm$^{-1}$. $\Delta\nu_0^v$ refers to the difference between the band origin in this work and Ref. [10].

| | | | | | Perturbing levels | | | |
|---|---|---|---|---|---|---|---|---|
| $v'$ | $\nu_0^v$ | $\Delta\nu_0^v$ | $B_v$ | $D_v$ | $v_{\text{pert}}^{\prime C}$ | $W_{BC}$ | $v_{\text{pert}}^{\prime EF}$ | $W_{BEF}$ |
| 19 | 108 001.56(1) | +1.62 | 7.840(2) | $0.065(5)\times10^{-2}$ | | | | |
| 18 | 107 276.61(1) | +0.27 | 8.175(1) | $0.119(4)\times10^{-2}$ | 4 | 3.81(2) | | |
| 17 | 106 529.59(2) | +0.62 | 8.487(2) | $0.42(2)\times10^{-2}$ | 4 | 6.20(2) | 12 | 1.0(2) |
| 16 | 105 764.37(1) | +0.12 | 8.68(1) | $0.26(3)\times10^{-2}$ | | | | |
| 14 | 104 168.22(1) | +0.07 | 9.172(3) | $0.24(1)\times10^{-2}$ | | | 8 | 6.6(1) |
| 13 | 103 337.3(1) | +0.0 | | | | | | |
| 12 | 102 484.38(1) | −0.44 | 9.745(5) | $0.40(3)\times10^{-2}$ | | | 5 | 5.01(2) |

perturbations. Even more important is that, in 1 xuv +1 uv photoionization detection of hydrogen, the line intensities are known to be strongly affected by autoionizing resonances in the continuum [18]. In the present analysis previous identifications [10] were taken as a starting point. Term values for the rovibrational states were calculated from the molecular constants of Dabrowski and Herzberg [10] and plotted in Fig. 4 to obtain an indication for the occurrence of local perturbations. In this term value plot locations of nonadiabatic coupling effects between $B\,^1\Sigma_u^+$ and $C\,^1\Pi_u$ states are marked by rectangles. Since these rotation-electronic couplings scale with $J(J+1)$ [7], the effects are largest for increasing $J$. For HD also couplings of $B\,^1\Sigma_u^+$ and $C\,^1\Pi_u$ states with the

$EF\,^1\Sigma_g^+$ state are expected and the locations that will be most strongly affected are marked by an elliptically shaped frame. Because the total Hamiltonian commutes with $\hat{J}^2$, perturbations will only occur between states of equal $J$.

In the absence of interactions term values of rovibrational states can be expressed as

$$E_\nu(J) = \nu_{0\nu} + B_\nu[J(J+1) - \Lambda^2] - D_\nu[J(J+1) - \Lambda^2]^2, \tag{1}$$

with $\Lambda = 1$ for the $C\,^1\Pi_u$ state and $\Lambda = 0$ for the $B\,^1\Sigma_u^+$ and $EF\,^1\Sigma_g^+$ states. Perturbed energy levels are then expressed as eigenvalues of a matrix for each value of $J$ of the form

$$M(J) = \begin{bmatrix} E_\nu^B(J) & W_{B,C}\sqrt{J(J+1)} & W_{B,EF} & \cdots \\ W_{B,C}\sqrt{J(J+1)} & E_\nu^C(J) & W_{C,EF}\sqrt{J(J+1)} & \cdots \\ W_{B,EF} & W_{C,EF}\sqrt{J(J+1)} & E_\nu^{EF}(J) & \cdots \\ \cdots & \cdots & \cdots & \cdots \end{bmatrix}, \tag{2}$$

where the parameters $W_{i,j}$ denote the interaction parameters between mutually perturbing states. The coupling between the $B\,^1\Sigma_u^+$ and $EF\,^1\Sigma_g^+$ states is homogeneous and thus the matrix element is $J$ independent, whereas the interaction be-

tween $C\,^1\Pi_u$ and $EF\,^1\Sigma_g^+$ and the interaction between the $C\,^1\Pi_u$ and $B\,^1\Sigma_u^+$ states are heterogeneous, giving $J$-dependent matrix elements [19]. The size of the matrix is determined by the number of vibronic states that need to be

TABLE V. Band origin $\nu_0^v$, rotational constants $B_v$, $D_v$, and perturbation parameters in the $C\,^1\Pi_u$ state of HD, as calculated from the analysis. The value in parentheses represents the uncertainty in the last digit. All values are in cm$^{-1}$. $\Delta\nu_0^v$ refers to the difference between the band origin in this work and Ref. [10].

| | | | | | Perturbing levels | | | |
|---|---|---|---|---|---|---|---|---|
| $v'$ | $\nu_0^v$ | $\Delta\nu_0^v$ | $B_v$ | $D_v$ | $v_{\text{pert}}^{\prime B}$ | $W_{BC}$ | $v_{\text{pert}}^{\prime EF}$ | $W_{CEF}$ |
| $4\Pi^-$ | 106 711.47(3) | −0.07 | 18.957(6) | $0.95(2)\times10^{-2}$ | | | | |
| $4\Pi^+$ | 106 711.87(1) | | 19.348(9) | $1.35(3)\times10^{-2}$ | 17 | 6.20(2) | 12 | 0.40(30) |
| | | | | | 18 | 3.82(2) | 13 | |
| $2\Pi^-$ | 103 180.52(3) | +0.05 | 20.918(3) | $1.00(1)\times10^{-2}$ | | | | |

TABLE VI. Band origin $\nu_0^v$, rotational constants $B_v$, $D_v$, and deperturbation parameters in the $EF^1\Sigma_g^+$ state of HD, as calculated from the analysis. The value in parentheses represents the uncertainty in the last digit. All values are in cm$^{-1}$. $\Delta\nu_0^v$ refers to the difference between the band origin in this work and Ref. [10].

| | | | | | Perturbing levels | | | |
|---|---|---|---|---|---|---|---|---|
| $v'$ | $\nu_0^v$ | $\Delta\nu_0^v$ | $B_v$ | $D_v$ | $v'^B_{\text{pert}}$ | $W_{BEF}$ | $v'^C_{\text{pert}}$ | $W_{CEF}$ |
| 13 | 107 124.91(2) | +0.41 | 9.053(9) | | | | 4 | |
| 12 | 106 551.63(1) | +0.05 | 9.899(5) | $1.89(2)\times10^{-2}$ | 17 | 1.0(2) | 4 | 0.4(3) |
| 8 | 104 329.15(2) | +0.14 | 5.39(5) | $1.03(2)\times10^{-2}$ | 14 | 6.6(1) | | |
| 5 | 102 577.02(1) | −0.02 | 4.430(5) | $0.15(1)\times10^{-2}$ | 12 | 5.01(2) | | |

included in an analysis. For example, the $B$ $^1\Sigma_u^+$, $v = 18$ and 17 states both interact with $C$ $^1\Pi_u$, $v = 4$, while $B$ $^1\Sigma_u^+$, $v = 17$ perturbs $EF$ $^1\Sigma_g^+$, $v = 12$. As indicated in Fig. 4, also $B$ $^1\Sigma_u^+$, $v = 18$ is expected to interact with $EF$ $^1\Sigma_g^+$, $v = 13$, but the interaction strength turned out to be negligibly small. So in this example a $4\times4$ matrix has to be diagonalized for each $J$.

The energy levels of the $X$ $^1\Sigma_g^+$ ground state of HD are expressed by

$$E_G(J) = B_G J(J+1) - D_G J^2(J+1)^2 + H_G J^3(J+1)^3. \qquad (3)$$

The most accurate molecular constants reported in the literature are those of Essenwanger and Gush [20], obtained from pure rotational electric-dipole absorption measurements: $B_G = 44.6614(21)$ cm$^{-1}$, $D_G = 0.002\,558(6)$ cm$^{-1}$, and $H_G = 0.0174(5)\times10^{-4}$ cm$^{-1}$, where the values in parentheses correspond to $3\sigma$ uncertainties. For example, for the $J = 5$ state the uncertainties add up to less than 0.02 cm$^{-1}$ at a $1\sigma$ level. For lower $J$ the error is smaller and since the estimated errors for the xuv transitions are greater than or equal to 0.03 cm$^{-1}$, the ground-state energy levels were fixed at the values calculated from the constants of Essenwanger and Gush in the fitting procedures of the excited state energies.

Molecular constants for the excited states are determined from separate least-squares fitting routines that included all mutually perturbing rovibronic states at a time. For the $\Pi_{(f)}$ levels of the $C$ $^1\Pi_u$ state a separate analysis was performed for each vibrational level. The resulting molecular constants and coupling parameters are presented in Tables

IV–VI for the $B$ $^1\Sigma_u^+$, $C$ $^1\Pi_u$, and $EF$ $^1\Sigma_g^+$ states, respectively. In all cases but one a successful deperturbation analysis could be performed. The calculated frequency positions are compared with those observed and deviations are listed as $\Delta_{OC}$ in Tables I–III. The mean value of the deviations $\Delta_{OC}$ is 0.02 cm$^{-1}$, which illustrates that the average observational uncertainty of 0.035 cm$^{-1}$ is not underestimated. As a result, it is found that the $g, u$ symmetry-breaking coupling effect between the $B$ $^1\Sigma_u^+$ and $EF$ $^1\Sigma_g^+$ states is particularly strong in the case of $B$, $v = 12$ and $EF$, $v = 5$ states. Here the $J = 4$ level of $EF$, $v = 5$ is shifted by 1.75 cm$^{-1}$.

We observed a yet unassigned weak line at 103 221.6(1) cm$^{-1}$. Dabrowski and Herzberg [10] observed a line at the same frequency and assigned it as the $R(5)$ line of $B$-$X(14,0)$ band. If this line would be included as $R(5)$ in our deperturbation analysis its frequency would be 5.5 cm$^{-1}$ off and therefore we left it unassigned. Other weak lines were observed at 103 235.71(3) and at 103 229.3(5) cm$^{-1}$. In Ref. [10] a feature at 103 235.82 cm$^{-1}$ was assigned as the $P(2)$ line of the $EF$-$X(7,0)$ band. Calculation of the combination difference from the presently obtained data for $P(2)$ and $R(0)$ lines results in 267.86(4) cm$^{-1}$, which is outside the error limits of the expected difference (see below). So assignment of this feature as $P(2)$ of $EF$-$X(7,0)$ is not correct if the $R(0)$ is assumed to be properly assigned.

The combination of bands $EF$-$X(7,0)$ and $(6,0)$, $B$-$X(13,0)$, and $C$-$X(2,0)$ could not be deperturbed successfully. For these bands 34 data points are available (of which the $P$ lines cannot be considered independent) and a proper deperturbation analysis requires at least 15 parameters. The assignment of two $P(4)$-$R(2)$ pairs belonging to $B$-$X(13,0)$ and $EF$-$X(6,0)$ bands is not unambiguous because a deper-

TABLE VII. Energy splittings $\Delta J = 2$ in the $X$ $^1\Sigma_g^+$, $v = 0$ ground state of the HD molecule as obtained from the present work and from previous studies. In the studies of Essenwanger and Gush [20], Rich, Johns, and McKellar [22], and McKellar, Goetz, and Ramsay [23] a $3\sigma$ error was stated for the rotational constants and therefore the uncertainties in the energy splittings correspond to $3\sigma$. In the present work the mean deviation from a large set was determined and therefore the stated uncertainties also correspond to $3\sigma$. The uncertainties in the Raman data of Ref. [24] were multiplied by 3 to obtain a $3\sigma$ error. All values are in cm$^{-1}$.

| Reference | $\Delta(2\text{-}0)$ | $\Delta(3\text{-}1)$ | $\Delta(4\text{-}2)$ | $\Delta(5\text{-}3)$ |
|---|---|---|---|---|
| Present work | 267.07±0.025 | 443.10±0.04 | 616.14±0.05 | 785.03±0.04 |
| [20] | 267.051±0.012 | 443.062±0.024 | 616.084±0.025 | 785.007±0.035 |
| [22] | 267.070±0.011 | 443.09±0.06 | 616.15±0.19 | 785.21±0.58 |
| [23] | 267.073±0.010 | 443.082±0.025 | 616.09±0.06 | 784.99±0.13 |
| [24] | 276.09±0.06 | 443.08±0.06 | 616.09±0.06 | 784.99±0.06 |

turbation analysis cannot be made. The homogeneous and heterogeneous interactions between the three systems need to be included, while also the effect of interaction between the $EF$-states pertaining to the inner and outer well of the $EF$ double-well potential affects the location of energy levels. As can be seen in the energy-level diagram of Fig. 4, the rotational progressions of $EF\,{}^1\Sigma_g^+$, $v=6$ and 7 cross near $J=4$. Such phenomena were recently studied in $H_2$ by Ross and Jungen [21]. Although in this particular situation deperturbation was not successful, band origins of the ${}^1\Sigma^+$ states could be determined reliable from the $P(1)$ lines exclusively and the resulting values are included in Table IV. For some bands, $C$-$X$(5,0) and $EF$-$X$ (14,0), (11,0), and (10,0), not enough data were collected to perform a rotational analysis.

The present xuv excitation data can also be analyzed to yield accurate information on the $X\,{}^1\Sigma_g^+$, $v=0$ ground-state energy levels. The combination differences between $R(J)$ and $P(J+2)$ lines in the xuv spectra, corresponding to the energy separation between $(J+2)$ and $J$ levels in the ground state, are independent of the location and the perturbations in excited-state energy levels. The lowest difference $\Delta(2\text{-}0)$ was determined in 13 independent measurements [13 bands listed in Tables I–III for which both $R(0)$ and $P(2)$ were measured], each with an accuracy ranging from 0.04 to 0.07 cm$^{-1}$. Similarly, three higher combination differences $\Delta(3\text{-}1)$, $\Delta(4\text{-}2)$, and $\Delta(5\text{-}3)$ were determined multiple times. From a statistical averaging procedure a mean value and an uncertainty at $3\sigma$ level were determined for the four lowest combination differences. The values are listed in Table VII and compared with energy differences calculated from the molecular constants of Essenwanger and Gush [20] deduced from pure rotational electric-dipole transitions. Also, a comparison is given with two others sets of molecular constants, one obtained from measurements in the fundamental (1,0) infrared band [22] and one from the (3,0) to (6,0) overtone bands of HD [23]. Furthermore, data from rotational Raman spectroscopy [24] in which $\Delta J=2$ splittings in the ground state are measured directly are included.

The combination differences from the xuv excitation spectra are, within error limits, in agreement with all previous data on the $X\,{}^1\Sigma_g^+$, $v=0$ ground state. The presently obtained combination differences agree within $3\sigma$ with the most accurate values. The accuracy is better than in previous work, except for the high-quality data of Essenwanger and

Gush [20]. It is noted that in the present xuv study data are collected from a molecular beam with densities of about $10^{-5}$ Torr in the interaction zone. Therefore pressure shifts, commonly affecting the weak absorption features (when measured at high pressures), do not play a role in this study.

## IV. CONCLUSION

In the present work transition frequencies for a total of 147 lines in the $B\,{}^1\Sigma_u^+$–$X\,{}^1\Sigma_g^+$, $C\,{}^1\Pi_u$–$X\,{}^1\Sigma_g^+$, and $EF\,{}^1\Sigma_g^+$–$X{}^1\Sigma_g^+$ systems of HD were measured with a mean absolute accuracy of 0.035 cm$^{-1}$. This accuracy is a factor of 5 better than in previous work. The transition frequencies were treated in a semiempirical model assuming heterogeneous coupling between states of different orbital symmetry and homogeneous coupling between states of the same orbital symmetry. This deperturbation procedure failed in some details for the case where two vibrational levels of the $EF\,{}^1\Sigma_g^+$ state were involved. It shows that the treatment of the $EF\,{}^1\Sigma_g^+$ state as a single vibrational manifold is not correct. In fact, the adiabatic coupling between the inner well ($E$ state) and outer well ($F$ state), giving rise to perturbations, has to be included in a correct model. For $H_2$ this has recently been shown by Ross and Jungen [21], where $ab$ $initio$ and multichannel quantum-defect theory (MQDT) methods were employed to calculate energy levels in the double minimum $EF\,{}^1\Sigma_g^+$ state. Such a procedure is, however, outside the scope of the present study. The breaking of $g,u$ symmetry makes the problem for HD more complicated; in such a treatment interactions with $B\,{}^1\Sigma_u^+$ and $C\,{}^1\Pi_u$ states will have to be incorporated simultaneously with the MQDT calculations for the gerade states. Our accurate data provide a testground for future theoretical calculations.

Even for an analysis of the $X\,{}^1\Sigma_g^+$ ground state the present data for xuv excitation are important. Although data from pure rotational excitation are somewhat more accurate, this set of data provides additional proof of the correctness of previous work. Of importance is the fact that the xuv spectra are recorded at extremely low densities and under the collision-free circumstances of a molecular beam.

[1] W. Kolos and L. Wolniewicz, Rev. Mod. Phys. **35**, 473 (1963).

[2] W. Kolos and L. Wolniewicz, Can. J. Phys. **53**, 2189 (1975).

[3] L. Wolniewicz and K. Dressler, J. Chem. Phys. **85**, 2821 (1986).

[4] K. Dressler and L. Wolniewicz, J. Chem. Phys. **96**, 6053 (1992).

[5] I. Dabrowski, Can. J. Phys. **62**, 1639 (1984).

[6] P. C. Hinnen, W. Hogervorst, S. Stolte, and W. Ubachs, Can. J. Phys. **72**, 1032 (1994).

[7] P. S. Julienne, J. Mol. Spectrosc. **48**, 508 (1973).

[8] R. A. Durie and G. Herzberg, Can. J. Phys. **38**, 806 (1960).

[9] G. Herzberg, J. Mol. Spectrosc. **33**, 147 (1970).

[10] I. Dabrowski and G. Herzberg, Can. J. Phys. **54**, 525 (1976).

[11] J. M. Gilligan and E. E. Eyler, Phys. Rev. A **46**, 3676 (1992).

[12] D. Shiner, J. M. Gilligan, B. M. Cook, and W. Lichten, Phys. Rev. A **47**, 4042 (1993).

[13] A. Balakrishnan, M. Vallet, and B. P. Stoicheff, J. Mol. Spectrosc. **162**, 168 (1993).

[14] W. Ubachs, K. S. E. Eikema, and W. Hogervorst, Appl. Phys. B **57**, 411 (1993).

[15] P. C. Hinnen, W. Hogervorst, S. Stolte, and W. Ubachs, Appl. Phys. B **59**, 307 (1994).

[16] S. Gerstenkorn and P. Luc, *Atlas du Spectre d'Absorption de la Molecule de l'Iode* (CNRS, Paris, 1978).

[17] S. Gerstenkorn and P. Luc, Rev. Phys. Appl. **14**, 791 (1979).

[18] W. Meier, H. Rottke, H. Zacharias, and K. H. Welge, J. Chem. Phys. **83**, 4346 (1985).

[19] H. Lefebvre-Brion and R. W. Field, *Perturbations in the Spectra of Diatomic Molecules* (Academic, London, 1986).

[20] P. Essenwanger and H. P. Gush, Can. J. Phys. **62**, 1680 (1984).

[21] S. C. Ross and Ch. Jungen, Phys. Rev. A **50**, 4618 (1994).

[22] N. H. Rich, J. W. C. Johns, and A. R. W. McKellar, J. Mol. Spectrosc. **95**, 432 (1982).

[23] A. R. W. McKellar, W. Goetz, and D. A. Ramsay, Astrophys. J. **207**, 663 (1976).

[24] B. P. Stoicheff, Can. J. Phys. **35**, 730 (1957).